Polarforschung 67 (1/), 65 – 75, 1997 (erschienen 2000)

Energy and Mass Balance at the Surface in the Wet Snow Zone of Northeast Glacier, Antarctic Peninsula

By Christoph Schneider[1]

Summary: This paper investigates the mass balance of the snow cover in the wet snow zone and the energy balance during the summer on Northeast Glacier located at 67 °W and 68 °S in Marguerite Bay, Antarctic Peninsula. Three automatic weather stations (AWS) were operated on Northeast and the nearby McClary Glacier in summer 1994/95. Furthermore, snow cover characteristics and the snow cover development were observed by means of snow pits and ablation stakes. During the winter accumulation varies spatially to a high degree. Readings in snow pits and at ablation stakes give values between 300 mm and 400 mm of water equivalent. The ablation during summer time correlates with mean air temperature or altitude. In the lowermost parts of the glaciers, ablation is 200-400 mm of water equivalent. The observations show that an ablation zone developed on Northeast Glacier at the end of the summer 1994/95. The equilibrium line altitude then was at 110 m above sea level.
There was good agreement between the observed snow melt in summer and snow melt calculated from micro-meteorological measurements by means of energy balance computations. These show, that summertime energy balance at the surface of the snow cover is dominated by turbulent heat fluxes. Energy input to the snow cover mainly is due to energy gain by sensible heat flux. The combination of the turbulent heat fluxes governs the residual energy, which is available for snow melt. Therefore, snow melt is very much depending on the combination of air temperature, water vapour pressure and wind velocity. This is illustrated by three examples from January 1995, which represent typical synoptic situations on the west coast of the Antarctic Peninsula. It is shown that the most efficient snow melt occurs when warm and moist air from lower latitudes is transported to Marguerite Bay by winds from northern and western directions. Since different synoptic situations promote different ablation, the importance of synoptic climatology for investigating the glacier's response to climate forcing is stressed.
It is concluded that at coastal regions of the western Antarctic Peninsula further warming will lead to the formation of large ablation zones. In case of further warming, run-off from glaciers - as one part of the mass balance - will gain importance, because the albedo of bare glacier ice in these ablation zones is much lower than the albedo of wet snow. These changes in the snow cover have short-termed consequences in contrast to long-term adjustments of the glacial dynamic to climate variations.

Zusammenfassung: Es wird die Massen- und Energiebilanz der Schneedecke in der Nassschneezone des Northeast-Gletschers in der Marguerite Bay, Antarktische Halbinsel (67 °W, 68 °S) untersucht. Hierfür wurden im Sommer 1994/95 drei automatische Wetterstationen (AWS) auf dem Northeast- und dem nahegelegenen McClary-Gletscher betrieben. Zudem wurde der Zustand und die Entwicklung der Schneedecke mit Hilfe von Schneeschächten und Ablationsstangen erfasst. Die winterliche Akkumulation variiert räumlich sehr stark. Die Ablesungen in Schneeschächten und an den Ablationsstangen ergeben Werte von 300-400 mm Wasseräquivalent. Die Ablation im Sommer korreliert mit der mittleren Lufttemperatur beziehungsweise der Höhenlage. In den untersten Lagen der Gletscher beläuft sich die Ablation auf 200-400 mm Wasseräquivalent. Die Beobachtungen zeigen, dass sich am Ende des Sommers 1994/95 eine Ablationszone ausgebildet hatte. Die Gleichgewichtslinie lag bei 110 m über dem Meeresspiegel.

Es wurde eine gute Übereinstimmung erzielt zwischen der beobachteten Schneeschmelze im Sommer und der Schneeschmelze, wie sie mit Hilfe der Oberflächenenergiebilanz aus mikrometeorologischen Messungen abgeleitet wurde. Es zeigt sich, dass die sommerliche Energiebilanz durch die turbulenten Wärmeströme dominiert wird. Der Energieeintrag in die Schneedecke ist hauptsächlich durch den Gewinn an fühlbarer Wärme zu erklären. Das Zusammenwirken der turbulenten Wärmeströme bestimmt maßgeblich das Residuum, welches zur Schneeschmelze zur Verfügung steht. Deshalb ist die Schneeschmelze in hohem Maße abhängig von der Kombination von Lufttemperatur, Wasserdampfdruck und Windgeschwindigkeit. Dies wird an drei Beispielen aus dem Januar 1995 aufgezeigt, die typische Wetterlagen an der Westküste der Antarktischen Halbinsel repräsentieren. Es zeigt sich, dass die effektivste Schneeschmelze dann auftritt, wenn warme und feuchte Luft niederer Breiten bei Winden aus nördlichen und westlichen Richtungen in die Marguerite Bay geführt werden. Da die unterschiedlichen Witterungslagen zu unterschiedlicher Ablation führen, wird auf die Bedeutung der synoptischen Klimatologie bei der Untersuchung der Reaktion von Gletschern auf Klimaschwankungen hingewiesen.
Es wird geschlossen, dass eine weitere Erwärmung der küstennahen Regionen der westlichen Seite der Antarktischen Halbinsel im Sommer zur großflächigen Ausbildung von Ablationszonen führen wird. Im Falle weiterer Erwärmung wird der Abfluss von den Gletschern – als ein Teil der Massenbilanz – an Bedeutung gewinnen, da die Albedo der aperen Flächen in diesen Ablationszonen wesentlich geringer ist, als die Albedo des feuchten Schnees. Im Gegensatz zu langfristigen Anpassungen der Gletscherfließdynamik an Klimaschwankungen wirken sich die Veränderungen an der Schneedecke bereits kurzfristig auf den Massenhaushalt der Gletscher aus.

1. INTRODUCTION

The Antarctic Peninsula (Fig. 1), which comprises only 7 % of the Antarctic continent, receives 23 % of the annual precipitation of ANTARCTICA (DREWRY & MORRIS 1992). The west coast of the Peninsula is covered by a variety of small and medium-sized valley glaciers, outlet glaciers of the ice-shields of the plateau, piedmont-type glaciers and fringing glaciers (FLEMING et al. 1938, NICHOLS 1960). Furthermore, small ice shelves, e.g. Müller -,Wilkes -, King-George-VI- and Wordie Iceshelf, are supported by ice streams that flow down the western slopes of the mountain ridge. Meteorological records from the west coast of the Peninsula show a 2.5 K warming during the second half of the 20th century (SMITH & STAMMERJOHN 1996).

WARRICK et al (1996) point out, that two thirds of the projected rise in sea level during the next century can be attributed to the thermal expansion of the oceans and one third is due to melting of mountain glaciers and small ice caps. Antarctica and Greenland will contribute little to the sea level rise during that period, because of the very long response time of the great ice sheets to global change, and because of increasing precipitation in Antarctica in a warmer climate (Warrick et al. 1996). However,

[1] Institut für Physische Geographie, Universität Freiburg, Werderring 4, D-79085 Freiburg, Germany, <christoph.schneider@ipg.uni-freiburg.de>

Manuscript received 18 June 1999, accepted 18 December 1999

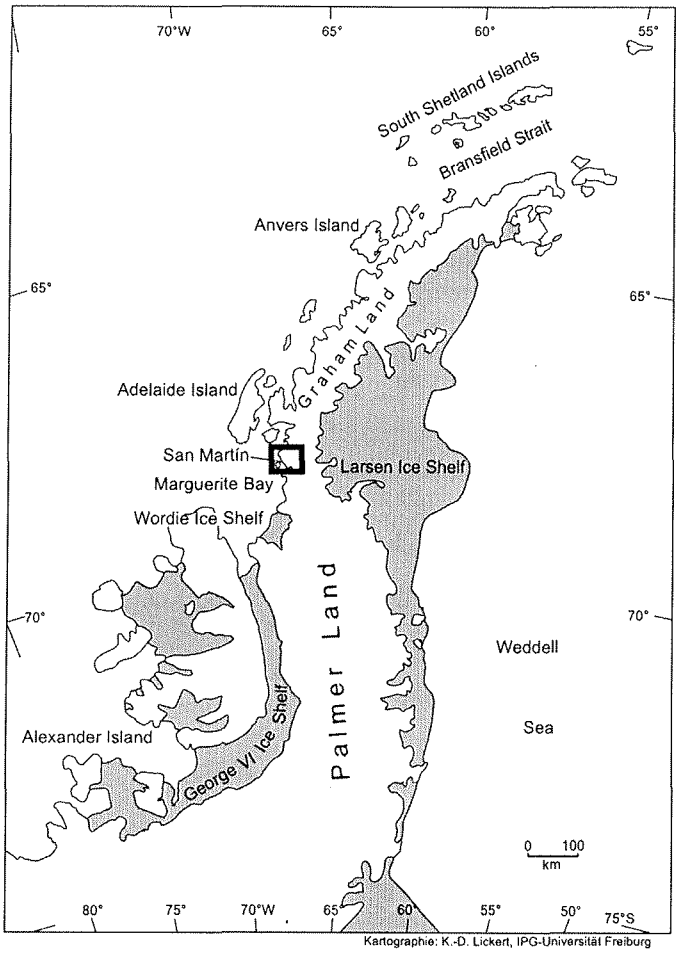

Fig. 1: Map of the Antarctic Peninsula. The study area covered by Figure 2 is indicated by a rectangle.

Abb. 1: Karte der Antarktischen Halbinsel. Die Lage des Untersuchungsgebietes (vgl. Abb. 2) ist durch ein Rechteck angegeben.

many glaciers in coastal parts of the Antarctica Peninsula experience considerable surface melting during the summer, which directly contributes to the run-off into the sea. In addition, the response of these small glaciers to climate forcing takes place only within decades. Consequently, the glaciers of the Antarctic Peninsula must not be neglected when global sea level rise is considered. In order to concretise the impact of melted snow and ice on sea level rise it is important to gather as much information as possible from the glaciated regions worldwide. For example, Drewry and Morris (1992) give a value of 0.012 mm a^{-1} K^{-1} as the contribution of the Antarctic Peninsula to sea level rise. Paren et al. (1993) derive values between 0.15 mm a^{-1} and 0.3 mm a^{-1} using different scenarios. Warrick et al. (1996) estimate the global contribution of melted snow and ice to sea level rise to 1.6 mm a^{-1}.

This study aims at presenting information on the energy balance in summer and the annual surface mass balance of the coastal parts of Northeast Glacier in Marguerite Bay on the west coast of the Peninsula. It does not further address the topic of the Antarctic Peninsula's contribution to sea level rise. However, it is anticipated that extended information on ablation and mass balance from different coastal areas of the Peninsula may help improving the estimation of the glaciers' future response to climate variations. The details presented in this paper extent what has already been published in Schneider (1999) in respect to the mass balance of the snow surface as well as to the sensitivity of the energy balance to specific meteorological conditions.

Up to now only few studies have focussed on small glaciers of the Antarctic Peninsula. Besides studies from the South Shetland Islands (Noble 1965, Jiahong et al. 1994, Ren Jiawen 1995, Bintanja 1995, Jiahong et al. 1998) investigations were published on the mass balance of Anvers Island (Rundle 1969, Casassa 1989), the energy and mass balance of Spartak Glacier on Alexander Island (Jamieson & Wagner 1983), the mass balance of an ice ramp at Rothera Point (Smith et al. 1998) and the spatial distribution of the wet snow zone in summer on Northeast Glacier derived from radar satellite imagery (Wunderle 1996). Investigations by Braun & Schneider (1999) reveal that the energy and mass balance on small glaciers show distinct differences between Marguerite Bay and the South Shetland Islands. This is in agreement with the more maritime climate in the north-west parts of the Antarctic Peninsula when compared to the continentally toned climate south of Adelaide Island. Marguerite Bay indicates the transition zone between northerly and southerly climate of the western Antarctic Peninsula (Reynolds 1981, Harangozo et al. 1997).

2. STUDY AREA

Northeast Glacier

The Northeast Glacier (Fig. 2) is located at 68°07' South and 67°00' West in Marguerite Bay close to Stonington Island (former base of the British Antarctic Survey) and the Argentine Base "San Martín" on Barry Island. First observations were made as early as the thirties and forties of the 20th century by the British Antarctic Survey (Rymill 1939, Skinner 1970) and the Ronne Antarctic Expedition (Ronne 1945, Knowles 1945). It is an outlet glacier of the plateau fed by an ice fall coming down from about 1500 to 550 m a.s.l. (Fig. 3). Downstream, Northeast Glacier develops into a 20 km long valley glacier which experiences a piedmont-like widening near the coast. The glacier tongue is never afloat. Between Cape Calmette and the Roman Four Promontory it forms - together with the McClary Glacier - a 12 km long ice cliff which runs approximately from Northwest to Southeast (Fig. 4). Bathymetric data between Barry Island (San Martín) and Stonington Island indicate a glacial trough near Stonington Island. The ice thickness near the ice cliff is estimated to vary between 80 m and 200 m (Schneider 1999). Flow velocity near the coast spatially varies between less than 10 m/year near Barry Island and about 150 m/year in the central parts of Northeast Glacier (Knowles 1945, Nichols 1960, Wunderle & Schmidt 1998).

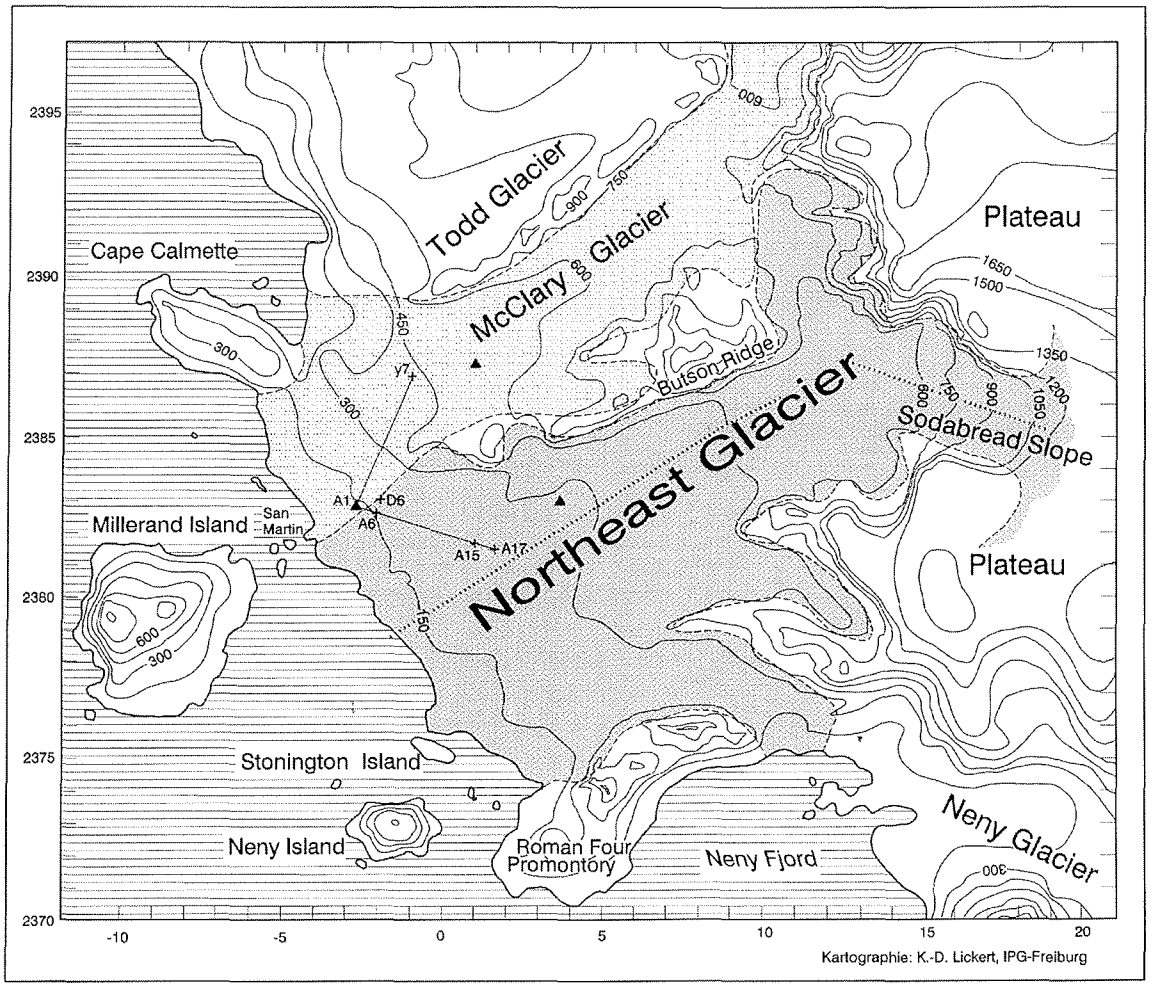

Fig. 2: Map of the study area derived from a digital elevation model (IfAG Frankfurt). Shaded areas denote the surface of Northeast Glacier and McClary Glacier. The map is based on a stereographic projection. The central meridian (67 °W) obtains 0.0 on the X-axis. The numbers are in km. The numbers on the Y-axis give the distance to the south pole. The northern boundary of the map corresponds approximately 68 °S. The triangles denote the locations of the AWSs during the summer campaign 1994/1995. The lines A1 to y7 and A1 to A17 indicate the profile lines of the ablation stakes. All measurements referring to the "measuring field" were derived from locations between A1, A6 and D6. The profile line along Northeast Glacier (Fig. 3) is indicated by a dotted line.

Abb. 2: Karte des Untersuchungsgebietes abgeleitet aus einem digitalen Geländemodell des IfAG, Frankfurt. Die schattiert dargestellten Flächen zeigen die Oberfläche von Northeast- und McClary-Gletscher. Die Karte beruht auf einer stereographischen Projektion. Der zentrale Meridian (67 °W) erhielt die Nullmarke des Gitters. Die Zahlenangaben sind in Kilometer. Die Zahlenangaben an der y-Achse stellen den Abstand vom Südpol dar. Der nördliche Kartenrand entspricht ungefähr 68 °S. Die Dreiecke markieren die Standorte der AWS während der Sommerkampagne 1994/1995. Die Linien von A1 nach Y7 und von A1 nach A17 stellen die Profillinien aus Ablationsstangen dar. Alle Messungen, die sich auf das zentrale "Messfeld" beziehen, wurden zwischen den Punkten A1, A6 und D6 gewonnen. Das Profil entlang des Northeast-Gletschers ist durch eine gepunktete Linie angezeigt.

Regional Climate

The climate of Marguerite Bay marks the transition from moist and moderate climate further north to the continentally toned climate in the south and east. The mean annual temperature at San Martín is -5.7 °C (WUNDERLE 1996). The monthly temperature minima are shifted towards the late winter, because of the annual sea ice in the bay. Surrounded by high mountains, Alexander Island in the south, the mountain ridge of the Peninsula in the east and Adelaide Island in the north, Marguerite Bay receives a high quantity of sunny days because of its sheltered location. Between 1945 and 1950 Stonington Island in Marguerite Bay received twice as much sunny days per year (38) as Base Faraday, which is located south of Anvers Island (PEPPER 1945). Weather patterns in Marguerite Bay are predominated by the alternation of warm north-westerly airflow and cold southerlies. Moist and warm air is advected pre-frontally when cyclones approach the Peninsula from the Bellingshausen Sea. Even in mid-winter during these weather situations the air temperature occasionally rises above 0 °C (PETERSON 1948). Deep air pressure on the west coast often triggers foehn-type gales that suck cold and dry air masses from the southern Weddell Sea over the mountain chain of the Peninsula into Marguerite Bay. At high wind speeds, adiabatically warmed air masses with very low air humidity are then forced into Marguerite Bay, leading to high sublimation and strong wind drift on the glaciers near the coast

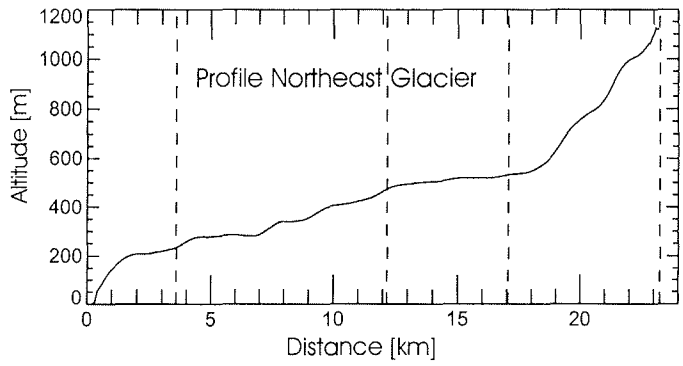

Fig. 3: Altitude of the glacier surface of Northeast Glacier along a profile line from the plateau down to the ice cliff. The profile is indicated in Figure 2 as a dotted line.

Abb. 3: Höhe der Gletscheroberfläche des Northeast-Gletschers entlang eines Profiles vom Plateau hinunter zur Kalbungsfront.

Fig. 4: View onto McClary Glacier (to the left) and the northern parts of Northeast Glacier (to the right). The photograph was taken from the northwest-facing slopes of Millerand Island (Fig. 2) The Argentinean base "San Martín" is hidden by Millerand Island on the right margin of the picture. (C. Schneider, January 1995).

Abb. 4: Sicht auf den McClary-Gletscher (links) und die nördlichen Teile des Northeast-Gletschers. Die Aufnahme wurde von der Nordwestflanke Millerand Islands aus (vgl. Abb. 2) aufgenommen. Die argentinische Station San Martín wird am rechten Bildrand durch Millerand Island verdeckt.

(SCHWERDTFEGER 1984). Precipitation at sea level at Northeast Glacier is estimated to be between 280-400 mm (PETERSON 1948, PEPPER 1954, SCHWERDTFEGER 1984). 80 % of the precipitation events in the northern Marguerite Bay are associated with northerly or westerly airflow (TURNER et al. 1995, Turner et al. 1997). Air temperatures at San Martín and Rothera Point are strongly correlated. As for the Faraday meteorological record, the Rothera Point temperature record shows a warming trend of 0.06 K a^{-1} (KING 1994) over the last four decades. FUCHS (1982) states that on Stonington Island and on the adjacent mountains the snow free areas in late summer were a lot larger in 1972/73 when compared to the situation of the 1940s. FOX & COOPER (1998) derive a similar result from the analysis of old aerial photographs dating back to 1956 from periglacial areas in the northern part of Marguerite Bay.

3. FIELD DATA

Field data from Northeast Glacier was gathered during two summer seasons. In 1993/94 WUNDERLE (1996) established a net of 45 ablation stakes to monitor accumulation and ablation patterns in the wet snow zone. The stakes were organised to cover a central field (between A1 and D6 in Fig. 2) and two profiles (A1 to A17 and A1 to Y7 in Fig. 2). Furthermore, data from snow pits was sampled and an automatic weather station (AWS) was operated from January 26th to March 2nd 1994. Readings of the ablation stakes were taken monthly by the winterers of the nearby Argentinean base San Martín.

From December 19th 1994 to February 21st 1995, three AWS (Campbell Scientific Ltd., UK), were operated on Northeast and McClary Glacier (small triangles in Fig. 2). The AWSs recorded net radiation (Q-7 net radiometer, Campbell Sci.), global solar radiation, reflected short-wave radiation (SP1110, Skye), wind speed (A100R, Campbell Sci.), wind direction, snow temperature at 20, 40 and 100 cm of snow depth (Type 107, Campbell Sci.), air temperature and air humidity (HMP35A, Vaisala) at 80 and 200 cm above ground in intervals of 10 seconds. All data were stored as means over 10 minutes. 40 snow pits were dug to cover the spatial and temporal variability of the snow cover. Parameters measured included the stratigraphy of the snow cover, snow grain size and type, temperature profile, hardness, humidity and snow density. Figure 5 for example, shows the snow pit from December 30th 1994 at the location ANT2 on McClary Glacier (Fig. 2).

4. MASS BALANCE

Annual precipitation at Stonington Island (see Fig. 2) amounts to between 300-400 mm (PEPPER 1954). In the snow pits (e.g. Fig. 5) summer and winter snow can be separated. After the summer season the snow in the upper 50 cm of the snow cover is denser because of the many melt-and-freeze events. Many ice lenses stratify this part of the snow cover. In Figure 5 one set of ice lenses and a local maximum of snow density which corresponds to a summer season, can be seen at a depth of 100 cm. A second summer can be identified because of a bundle of ice lenses at approximately a depth of 200 cm. The distinction between summer and winter season, which can be interpreted from single snow pits, can also be derived by plotting the relative frequency of ice lenses within intervals of 10 cm against snow depth. However, since many snow pits of one area were put into one graph, the peaks are very broad and only rough estimates of annual accumulation can be obtained. Figure 6a represents all snow pits obtained from McClary Glacier at altitudes varying between 400-550 m a.s.l.. Two broad peaks can be found with their maximums approximately at 90 cm signifying the summer of 1993/1994 and at 165 cm depth (summer 1992/93). Using a mean snow density of 450 kg/m^3 an accumulation of 405 mm a^{-1} can be calculated. Readings at the ablation stakes on McClary Glacier in summer 1994/95 return similar values for the total annual accumulation. The meteorological measurements and the snow pits reveal, that in summer there is no substantial decline of the snow cover at this altitude due to melting, although air temperature often exceeds 0 °C.

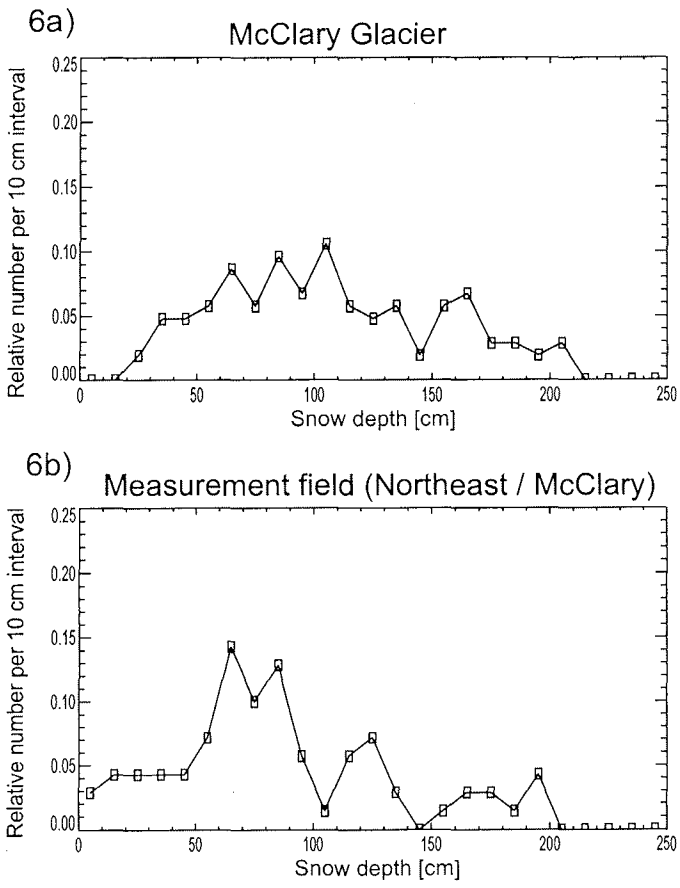

Fig. 6: Relative number of ice lenses per 10 cm of depth plotted against snow depth for all snow pits of the field campaign 1994/95 from McClary Glacier **(a)** and from the measuring field on Northeast Glacier / McClary Glacier **(b).**

Abb. 6: Relative Häufigkeit von Eislinsen pro Tiefenintervall von 10 cm. Die Größe ist gegen die Schneetiefe aufgetragen. Es wurden alle Schneeschächte der Messkampagne 1994/95 vom McClary-Gletscher **(a)** und vom Messfeld (Northeast- /McClary-Gletscher) **(b)** ausgewertet.

Figure 6b represents ice lenses found in snow pits in the vicinity of A1 (Fig. 2) at altitudes between 120-180 m a.s.l.. Three peaks at 75 cm, 120 cm and 185 cm separate two annual layers. These can be attributed to the winter of 1992 and the winter of 1993. The net accumulation amounts to 225 mm and 325 mm of water equivalent assuming a mean snow density of 500 kg/m^3.

The readings at the ablation stakes which cover the following year (1994) show that during wintertime (Fig. 7 left) the accumulation was about 360 mm (80 cm of snow height with 450 kg/m^3 of snow density). Readings at the same stakes at the end of the summer season of 1994/95 (Fig. 7 right) clearly show that no substantial decline of the snow cover due to melting took place at altitudes higher than approximately 300 m a.s.l.. The graph also shows that the equilibrium line's altitude was about 110 m a.s.l. at the end of the summer. The mean air temperature from November 1994 to February 1995 at San Martín was +1.2 °C. In contrast to the summer of 1994/95 no ablation zone developed in 1993/94. The mean summer air temperature in 1993/94 was -1.0 °C. WUNDERLE (1996) estimated the equilibrium line after that season to be approximately at sea level.

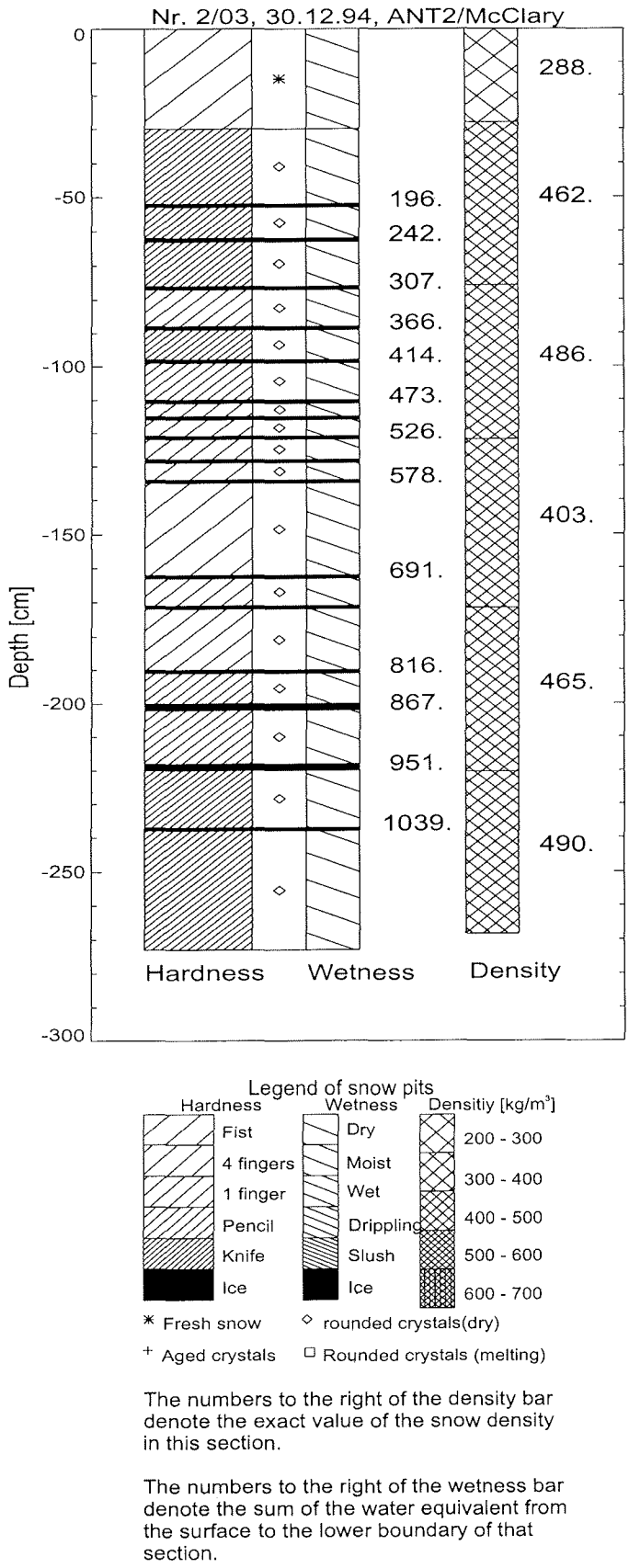

Fig. 5: Snow pit Nr.2/03 from 30/12/94 at the location of the AWS on McClary Glacier (small triangle in Fig. 2).

Abb. 5: Schneeschacht Nr. 2/03 vom 30/12/94 bei der AWS auf dem McClary-Gletscher (siehe kleines Dreieck in Abb. 2).

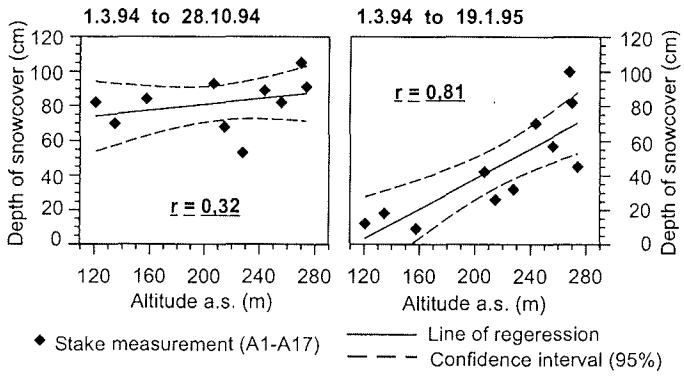

Fig. 7: Relation between snow height measured at ablation stakes and altitude of the ablation stake on the glacier. Single measurements are from the profile A1 to A17 (Fig. 2). The left plot shows snow accumulation between March 1st 1994 and October 28th 1994. The right plot includes most of the ablation in summer. It is based on readings from January 19th 1995.

Abb. 7: Beziehung zwischen an den Ablationsstangen gemessener Schneehöhen und der Höhenlage der Stangen. Die einzelnen Messungen entstammen dem Messprofil von A1 nach A17 (vgl. Abb. 2). Der linke Teil der Abbildung zeigt die Akkumulation zwischen dem 1. März 1994 und dem 28. Oktober 1994. Der rechte Teil der Abbildung schließt zusätzlich die sommerliche Ablation mit ein. Sie basiert auf Ablesungen vom 19. Januar 1995.

From the time series of snow pits in the summer 1993/94 at the location A1 at 120 m a.s.l. a total ablation of 315 mm can be calculated. The readings at the nearby ablation stake brought out a sum of 318 mm of ablation using snow density measurements. It was not possible to obtain more readings from the remaining ablation stakes before August 1996 due to logistical reasons. The mean of the snow height of all 16 remaining ablation stakes in the central field in February 1997 was 74 cm. This is equivalent to a net mass balance at the surface for both years together of 370 mm assuming a mean snow density of 500 kg/m³. Table 1 summarises the estimates of surface net mass balance in the measuring field of Northeast Glacier from 1992 to 1997 derived from different data sources.

Mass balance year	Net mass balance
1992/93	325
1993/94	225
1994/95	200
1995/96	185*
1996/97	185*

Tab. 1: Estimated mass balance of the snow cover in the wet snow zone of Northeast Glacier between 120 m and 160 m a.s.l. between 1992 and 1997. The values were derived from readings at ablation stakes and from snow pits. The two values labelled with * were derived in one single measurement for both years together.

Tab. 1: Abschätzungen der Massenbilanz der Schneedecke in der Nassschneezone des Northeast-Gletschers bei 120 m bis 160 m Höhe zwischen 1992 und 1997. Die Messungen wurden aus Ablesungen an Ablationsstangen und aus Schneeschachtaufnahmen abgeleitet. Die mit einem Stern gekennzeichneten Werte wurden in einer Einzelmessung für beide Massenhaushaltsjahre zusammen bestimmt.

From the different data sources presented it can be concluded that:

- Winter accumulation on the lowermost 500 m of McClary and Northeast Glacier amounts to about 300-400 mm of water equivalent.
- Ablation by snow melt during summer occurs between sea level and approximately 300 m a.s.l..
- The altitude of the equilibrium line mainly varies with the summer air temperature and the accumulation during the winter. While no ablation zone develops during chilly summers, it can be above sea level at the end of warm summers.

5. ENERGY BALANCE IN SUMMER 1994/95

The energy balance at the snow surface was computed from the recordings at the AWS. Since details to this topic have been published earlier (SCHNEIDER 1998a,b), only a summary of this analysis is presented here. When the energy input due to precipitation can be neglected, the energy budget equation can be simplified to

$$M = R + H + E \qquad (1)$$

with (M) the sum of the storage heat flux and the energy available for snow melt, (R) the net radiation, (H) the sensible heat flux and (E) the latent heat flux. During the field campaign, snow temperature was almost constantly at the melting point in the upper two meters of the snow cover. Therefore, the storage heat flux into the snow cover was negligible and the sum on the right side of (1) can be interpreted as the energy available for snow melt. Net radiation was measured directly at the AWS. Turbulent heat fluxes were measured according to the bulk approach formulations (OKE 1970, BRAITHWAITE 1995) taking into account the corrections due to stable stratification of the boundary layer by employing the bulk-Richardson number (BLACKADAR 1997, SCHNEIDER 1998a):

$$H = -\frac{\rho c_p \kappa^2 u(z)}{\ln\left(\frac{z}{z_{o,u}}\right)\ln\left(\frac{z}{z_{o,T}}\right)}\left(\Theta(z)-\Theta_o\right)(1-5Rb)^2 \qquad (2)$$

$$E = -\frac{\rho L_v 0.622 \kappa^2 u(z)}{p\left[\ln\left(\frac{z}{z_{o,u}}\right)\ln\left(\frac{z}{z_{o,q}}\right)\right]}\left(e(z)-e_o\right)(1-5Rb)^2 \qquad (3)$$

with:

ρ:	density of air
c_p :	specific heat at constant pressure of air
κ :	Van-Karman constant
u(z) :	wind velocity at screen-level
z :	screen level (200 cm)

$z_{0,u}$: roughness length for momentum
$\Theta(z)$: potential air temperature at screen level
$z_{0,T}$: surface roughness length for heat
Θ_0 : potential air temperature at the snow surface
Rb : bulk Richardson number
L_v : latent heat of evaporation or sublimation
p : air pressure
$z_{0,q}$: surface roughness length for water vapour
e(z) : water vapour pressure at screen level
e_0 : water vapour pressure at the surface (e_0 = 6.1 hPa)

For wind speeds lower than 3.5 m s^{-1} air temperature was corrected for the effect of radiative heating of the unventilated radiation shields using a formulation based on wind speed (u(z))

$$\Delta T = -\frac{I}{1080}\left(12.79e^{-4.02u(z)} + 0.33\right) \quad (4)$$

and short-wave irradiance (I) (SCHNEIDER 1998b).

This expression was derived from data supplied in a technical note by Young Company (MI, USA). From the energy balance computed according to (1), the actual snow melt was calculated using averages of one hour. This was compared to the observed decline of the snow cover using time series of snow pits. The snow pits were dug every 2 to 5 days depending on weather conditions. By this means the optimal values for the surface roughness lengths were derived and the systematic errors are compensated by constant off-sets of the surface roughness lengths. Since the surface roughness lengths were not derived from profile measurements the surface roughness lengths used in this study are fitted values and not parameters that merely reflect the mean physical condition of the snow surface. It turned out that the best agreement between modelled and measured snow melt (r = 0.9) was obtained using $z_{o,u} = z_{0,T} = 10^{-3}$ m and $z_{0,q} = 10^{-5}$ m. The much lower value of $z_{0,q}$ may be attributed to a systematic error of +2 % of relative humidtiy at the humidity probe at 2.0 m at the AWS. This can be deduced from the comparison between the humidity readings at 2 m and at 0.8 m above the surface. A 2 % error in the humidity reading would result in a 40 % overestimation of the latent heat flux. Reducing $z_{0,q}$ from 10^{-3} m to 10^{-5} m yields the contradictory effect of reducing latent heat flux by approximately 40 %. Although the overall agreement is very promising, there may be substantial deviations between modelled snow melt and actual snow melt for single measurements. The maximum error for the turbulent heat fluxes was estimated to ±22 % using an error propagation method and the radiation measurements are not supposed to be any better than ±15 % (SCHNEIDER 1998b). Therefore, the energy balance and the calculated snow melt have to be taken as estimates only. Merely, averages over at least a couple of hours should be compared. The total snow melt during the field campaign was computed to 375 mm water equivalent. This is in fair agreement with the ablation measured at the ablation stake nearby (312 mm), which may differ from the computed snow melt, because of the spatial dislocation of the two measurements, and because of the error resulting from the uncertainty of the snow density's exact values. The relative deviation between computed snow melt and the total depletion of the snow cover derived from the time sequence of snow–pits was 1 % only.

Weekly means of the terms of the energy balance from 20/12/94 to 21/02/95 are presented in Figure 8. Mean values for the total period are given in Table 2. A period with predominantly

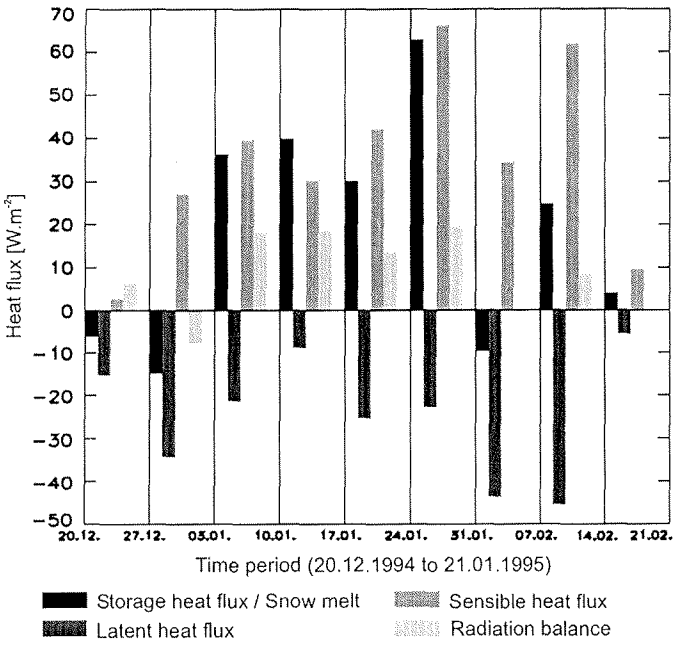

Fig. 8: Weekly means of the sensible heat flux, the latent heat flux and the radiation balance at the location A1 (see Fig. 2). The fourth column shows the residuum of the three other columns and can be interpreted as the energy input to the snow cover or its loss.

Abb. 8: Wochenmittel von fühlbarem Wärmestrom, latentem Wärmestrom und Strahlungsbilanz am Ort A1 (vgl. Abb. 2). Die vierte Spalte zeigt das Residuum der drei anderen Größen und kann als der Energieeintrag in bzw. der Energieaustrag aus der Schneedecke interpretiert werden.

Air temperature (2 m)	+0.8 °C
Wind speed (2 m)	4.6 m.s^{-1}
Relative humidity	70.1 %
Net radiation	8.6 W m^{-2} (46%)
Sensible heat flux	35.5 W m^{-2} (190%)
Latent heat flux	-25.5 W m^{-2} (-137%)
Turbulent heat fluxes	10.0 W m^{-2} (54%)
Total atmospheric heat flux	18.6 W m^{-2}

Tab. 2: Mean values of the terms of the energy balance and the meteorological readings for the period of observations from December 20th 1994 to February 21st 1995 at location A1 (Fig. 2).

Tab. 2: Mittelwerte der Energiebilanzterme und der meteorologischen Ablesungen während des Untersuchungszeitraumes vom 20. Dezember 1994 bis zum 21. Februar 1995 am Standort A1 (siehe Abb. 2).

negative energy balance during the first two weeks is followed by 4 weeks of intensive ablation. During the first week of February 1995, the snow surface experienced a slightly negative energy balance. The last two weeks of the field campaign show a positive energy balance, but the energy available for snow melt was much smaller than in January. The radiation balance was negative only in the second week of the field campaign. The major influence on the energy balance can be attributed to the turbulent heat fluxes. Energy input due to the sensible heat flux is about four times the radiation balance. However, the mean latent heat flux contributed to the energy loss from the snow surface by sublimation and evaporation. Opposite directions of the turbulent fluxes are unusual for melting ice surfaces in the ablation zone (see e.g. BINTANJA 1995, PATERSON 1994, p. 68 ff, GREUELL & KONZELMANN 1994, MALE & GRANGER 1981, DE LA CASINIÈRE 1974). Nevertheless, these can often be found in the wet snow zone, the percolation snow zone or just before the onset of summertime ablation with air temperatures near 0 °C combined with low air humidity (STEFFEN 1995, KONZELMANN & BRAITHWAITE 1995, JAMIESON & WAGNER 1983).

The radiation balance is a minor contributor to the overall energy turnover, because the high albedo of the snow of about 80 % significantly reduces the short-wave energy balance in comparison to bare glacier ice with an albedo of about 60 %. Furthermore, Marguerite Bay is surrounded by high mountains in the north (Adelaide Island), east (Antarctic Peninsula) and south (Alexander Island). Therefore, lee-side effects often reduce cloudiness. This yields a negative effect on the atmospheric long-wave radiation. The sum of the turbulent heat fluxes makes up 55 % of the snow surface's total energy gain in summer 1994/95. The contribution of the sensible heat flux itself is even higher because the mean latent heat flux is negative. This implies that a rise in air temperature does not necessarily need to trigger high ablation through enhanced sensible heat flux. Air humidity and wind velocity also have to be considered in detail. Therefore, it is of great interest to analyse the behaviour of the turbulent heat fluxes in different synoptic situations. Three examples representing distinct synoptic situations were chosen for illustration. A summary of the terms of the energy balance and other meteorological variables for each situation are given in Table 3.

From 15/01/95 to 17/01/95 a high pressure area that was centred above Alexander Island caused calm and sunny weather conditions in Marguerite Bay (Fig. 9a). A diurnal cycle of air temperature and radiation balance developed and only little wind - due to local wind systems - was observed. Although air humidity was low with only 53 % of relative humidity, the turbulent heat fluxes were rather small, because of the very small wind speed of only 2.4 m s^{-1} and low mean air temperature of +0.9 °C. Accumulated snow melt was only 7.6 mm.day^{-1} during this period of fine weather.

Strong winds and northerly to westerly winds were observed from 23/01/95 to 25/01/95. With a meso-cyclone moving towards east, warm and moist air masses from Northwest were advected to Marguerite Bay and occluded fronts passed (Fig. 9b). Since relative humidity was very high (73 %), the latent heat flux was small (-12 W m^{-2}). Unusual high average temperature of +3.1 °C in combination with strong wind (6.7 m s^{-1}) triggered high sensible heat flux (+78 W m^{-2}). Consequently, calculated snow melt was much higher than from January 15th to 17th with an average value of 21 mm day^{-1}.

The third synoptic situation from 30/01/95 and 31/01/95 (Fig. 9c) illustrates another common situation in Marguerite Bay: A cyclone was driven to the north-east, because of the mountains of the Antarctic Peninsula, and because of a high pressure area

	Period of fine Weather 15/01-17/01/95	Advection from NW 22/01-25/01/95	Foehn situation 30/01-31/01/95
Energy available for snow melt [W m^{-2}]	+42	+78	+3
Latent heat flux [W m^{-2}]	-15	-12	-125
Sensible heat flux [W m^{-2}]	+50	+78	+106
Net radiation [W m^{-2}]	+12	-11	+21
Air temperature [°C]	+0.9	+3.1	+1.9
Relative humidity [%]	53	72	50
Wind velocity [m s^{-1}]	2.4	6.8	14.5
Snow melt per day [mm]	8	21	5

Tab. 3: Summary of mean values of the terms of the energy balance and of the meteorological variables for three synoptic situations in January 1995. Details on the synoptic situations are presented in the text. The synoptic charts are given in Figure 9.

Tab. 3: Mittelwerte der Terme der Energiebilanz und einiger meteorologischer Variablen für drei ausgewählte Wittterungsperioden Abb. 9.im Januar 1995. Die Details zu den Witterungsperioden sind im Text ausgeführt. Die zugehörigen synoptischen Karten zeigt Abbildung 9.

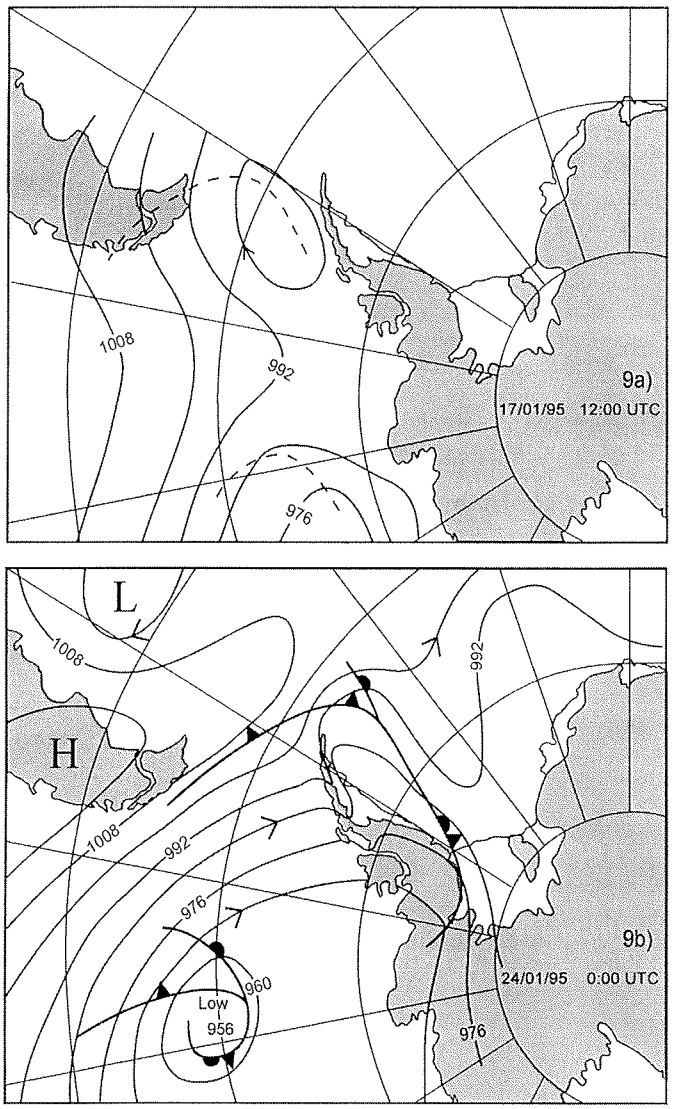

Fig. 9: Synoptic charts compiled from synoptic map of the British Antarctic Survey produced at Rothera base from January 1995. The three situations documented are: **(a)** a period of mostly fine weather and high pressure without cyclones in the vicinity of Marguerite Bay (January 17th 1995), **(b)** a situation with the advection of moist and warm air mass to Marguerite Bay in front of occluded cyclones moving eastwards from the Bellingshausen Sea (January 24th 1995), and **(c)** a cyclone moving towards Northeast along the Antarctic Peninsula. During this period, strong foehn-winds occurred in the study area, because of the low pressure area west of the mountains and higher air pressure over the Weddell Sea (January 30th 1995).

Abb. 9: Synoptische Karten verändert nach synoptischen Karten der Station Rothera des British Antarctic Survey vom Januar 1995. Die drei dokumentierten Wetterlagen zeigen: **(a)** eine Witterungsperiode mit überwiegend ruhigem Hochdruckwetter ohne zyklonale Störungen im Bereich der Marguerite Bay, **(b)** eine Situation mit der Advektion warmer und feuchter Luftmassen in die Marguerite Bay vor okkludierten Zyklonen, die von Osten über die Bellingshausen-See herannahen, **(c)** und eine Zykone, die entlang der Antarktischen Halbinsel nach Nordwesten zieht. Während dieses Zeitraumes traten, aufgrund des tiefen Drucks im Westen und höherem Druck über der Weddellsee, starke Föhnwinde im Untersuchungsgebiet auf.

over the Weddell Sea. Low air pressure on the west side of the Peninsula and high pressure in the east forced foehn winds over the ridge of the Antarctic Peninsula. At Northeast Glacier a gale with mean wind velocity of 14.5 m s^{-1} and wind direction from east occurred. Air humidity was extraordinarily low (50 %), because of the adiabtic warming of the air that descended the slopes of the mountains. The latent heat flux of -125 W m^{-2} caused strong sublimation of the snow cover. Although the air temperature was positive (+1.9 °C), in average not much snow melt could be observed, because the available energy was consumed by the sublimation process. The depletion of the snow cover of 4 mm day^{-1} can almost totally be attributed to the sublimation.

The three examples presented show, that the ablation in Marguerite Bay not only depends on the air temperature, but it also is sensitive to water vapour pressure and wind speed. Most efficient snow melt can be expected during synoptic situations that drive warm and moist air masses from north-west to Marguerite Bay.

7. CONCLUSION

The study conducted in Marguerite Bay on Northeast Glacier in 1994 and 1995 confirms, that monitoring of the snow cover can improve the understanding of local climate variability and its consequences on local glaciers. Snow accumulation in winter varies between 300-400 mm on the lowermost parts of Northeast Glacier. Summertime ablation exceeds 300 mm of water equivalent at 100 m a.s.l. during warm summers. It is expected, that as a feedback to regional climate warming the development or substantial enlargement of ablation zones is initiated. The albedo is very much lowered when the snow cover is completely removed, which again enhances ablation. Since large portions of the piedmont-type glaciers are located at altitudes below 500 m a.s.l., this will considerably raise direct run-off to the sea.

The energy balance at the snow surface of the wet snow zone of Northeast Glacier in summer is driven by variations of both of the turbulent heat fluxes. In this respect, it is important to monitor both, the air temperature and the air humidity, because of the important contribution of the latent heat transfer to the

total energy balance. Highest values of snow melt are obtained, when warm and moist air is advected, because this reduces energy loss due to latent heat flux and enhances the input from sensible heat. Although very dry air masses enhance evaporation or sublimation of the snow, the total loss from the snow cover is small, because snow melt is significantly reduced . The advection of air masses with distinct characteristics of air humidity and air temperature depend on the synoptic situation. Therefore, emphasis should be put on the relation between inter-annual climate variability inferred from meteorological records and the inter-annual variability of the occurrence of synoptic systems.

8. ACKNOWLEDGEMENTS

This research was supported by the German Secretary of Science and Research (BMBF) within the programme "Dynamic Processes in Antarctic Geosystems" (DYPAG) (Contract Number: 03PL016A) and by the ESA pilot study "Monitoring Of Dynamic Processes in Antarctic Geosystems" (MODPAG), (Contract Number: AO2.D149). The author would like to thank the Instituto Antarctico Argentino (IAA), the British Antarctic Survey (BAS) and the German Alfred-Wegener-Institut für Polar- und Meeresforschung (AWI) for their support with respect to logistics and field equipment. The author is grateful for the invaluable assistance and discussions in the field provided by M. Braun, S. Meissner, F. Rau, F. Weber and the Argentinean partners. The author is thankful to Stefan Wunderle who made available field data and remote sensing data from the summer campaign 1993/1994. The helpful comments of E. Parlow, C. Kottmeier and H. Habenicht are appreciated.

References

Bintanja, R. (1995): The local energy balance of the Ecology Glacier, King George Island, Antarctica: measurements and modelling.- Ant. Sci. 7: 315-325.

Blackadar, A.K. (1997): Turbulence and diffusion in the atmosphere.- Springer-Verlag, Berlin, Heidelberg.

Braithwaite, R.J. (1995): Aerodynamic stability and turbulent sensible-heat flux over a melting ice surface, the Greenland ice sheet.- J. Glaciol. 41: 562-571.

Braun, M. & Schneider, C. (in press): Characteristics of summertime energy balance along the west coast of the Antarctic Peninsula.- Ann. Glaciol. 30:

Casassa, G. (1989): Velocity, heat budget and mass balance at Anvers Island Ice Cap, Antarctic Peninsula.- Ant. Rec. 33: 341-352.

De La Casinière, A.C. (1974): Heat exchange over a melting snow surface.- J. Glaciol. 13: 55-72.

Fuchs, V. (1982): Of ice and men - the story of the British Antarctic Survey.- BAS Printers Limited, Over Wallop, England.

Drewry, D.J. & Morris, E.M. (1992): The response of large ice sheets to climatic change.- Phil. Trans. Roy. Soc. London 338: 235-242.

Fleming, W.L.S., Stephenson, A., Roberts, B.B. & Bertram, G.C.L. (1938): Notes on the scientific work of the British Graham Land expedition. 1934-37.- Geogr. J. Roy. Geogr. Soc. 91: 508-532.

Fox, A.J. & Cooper, A.P.R. (1998): Climate-change indicators from archival aerial photography of the Antarctic Peninsula.- Ann. Glaciol. 27, 636-642.

Greuell, W. & Konzelmann, T. (1994): Numerical modelling of the energy balance and the englacial temperature of the Greenland Ice sheet. Calculations for the ETH-Camp location (West Greenland, 1155 m a.s.l.).- Glob. Planet. Change 9: 91-114.

Harangozo, S.A., Colwell, S.R. & King, J.C. (1997): An analysis of a 34-year air temperature record from Fossil Bluff (71°S, 68°W), Antarctica.- Ant. Sci. 9: 355-363.

Jamieson, A.W. & Wager, A.C. (1983): Ice, water and energy balances of Spartan Glacier, Alexander Island.- Brit. Ant. Survey. Bull. 52: 155-186.

Jiahong, W., Jiancheng, K., Jiankang, H., Zichu, X., Leibao, L. & Dali, W. (1998): Glaciological studies on the King George Island ice cap, South Shetland Islands, Antarctica.- Ann. Glaciol. 27: 105-109.

Jiahong, W., Jiancheng, K., Zichu, X., Jiankang, H. & Lluberas, A. (1994). Climate, mass balance and glacial changes on small dome of Collins Ice Cap, King George Island, Antarctica.- Ant. Res. 5: 52-61.

Jiawen, R., Dahe, Q., Petit, J.R., Jouzel, J., Wenti, W., Chen, L., Xiaojun, W., Songlin, Q. & Xiaoxiang, W. (1995): Glaciological studies on Nelson Island, South Shetland Islands, Antarctica.- J. Glaciol. 41: 408-412.

King, J.C. (1994): Recent climate variability in the vicinity of the Antarctic Peninsula.- Int. J. Clim. 14: 357-369.

Knowles, P.H. (1945): Glaciology of southern Palmer Peninsula, Antarctica.- Proc. Amer. Phil. Soc. 89: 174-176.

Konzelmann, T. & Braithwaite, R.J. (1995): Variations of ablation, albedo and energy balance at the margin of the Greenland ice sheet, Kronprins Christian Land, eastern north Greenland.- J. Glaciol. 41: 174-182.

Knowles, P.H. (1945): Glaciology of southern Palmer Peninsula, Antarctica.- Proc. Amer. Phil. Soc., 89: 174-176.

Male, D.H. & Granger, R.J. (1981): Snow surface energy exchange.- Water Resouces Res. 17: 609-627.

Moore, R.D. (1983): On the use of bulk aerodynamic formulae over melting snow.- Nordic Hydr: 193-206.

Nichols, R.L. (1960): Geomorphology of Marguerite Bay area, Palmer Peninsula, Antarctica.- Bull. Geolog. Soc. Amer. 71: 1421-1450.

Noble, H.M. (1965): Glaciological observations at Admirality Bay, King George Island, in 1957-58.- Brit. Ant. Survey Bull. 5: 1-11.

Oke, T.R. (1970): Turbulent transport near the ground in stable conditions.- J. Appl. Met. 9: 778-786.

Paren, J.G., Doake, C.S.M. & Peel, D.A. (1993) The Antarctic Peninsula contribution to future sea level rise.- In: R.A. WARRIKCK, E.M. BARROW. & T.M.L. WIGLEY (eds.), Climate and sea level change; observations, projections and implications. Cambridge Uni. Press, Cambridge, 162-168.

Paterson, W.S.B. (1994): The physics of glaciers. – 3rd ed., Elsevier Kidlington, New York.

Pepper, J. (1954): The meteorology of the Falkland Islands and dependencies 1944 - 1950.- C. F. Hodgson and Son LTD, London.

Reynolds, J.M. (1981): The distribution of mean annual temperatures in the Antarctic Peninsula.- Brit. Ant. Survey Bull. 54: 123-131.

Ronne, F. (1945): The main southern sledge journey from East Base, Palmer Land, Antarctica.- Proc. Amer. Phil. Soc. 89: 13-22.

Rundle. A. (1969): Snow accumulation and ice movement on the Anvers Island ice cap, Antarctica: a case study of mass balance.- Proc. Int. Symp. Antarctic Glaciol. Explor., Dartmouth, N.H., Cambridge, 377-390.

Rymill, J.R. (1938): British Graham Land Expedition, 1934-37 - part II.- Geogr. J. Roy. Geogr. Soc. 91: 425-438.

Schneider, C. (1998a): Monitoring climate variability on the Antarctic Peninsula by means of observations of the snow cover.- Ann. Glaciol. 27: 623-627.

Schneider, C. (1998b): Zur raumzeitlichen Differenzierung der Energiebilanz und des Zustandes der Schneedecke auf zwei Gletschern der Marguerite Bay, Antarktische Halbinsel - Aspekte des Klimas und des Klimawandels am Rande der Antarktis.- Freiburger Geogr. Hefte 56, Institut für Physische Geographie, Universität Freiburg, Germany, Freiburg.

Schneider, C. (1999): Energy balance estimates during the summer season of glaciers of the Antarctic Peninsula.- Global Planet. Change 22: 117-130.

Skinner, A.C. (1970): Field report on the geology of the Mount Wilcox area, between Calmette and Square Bay Coasts, McClary and Swithinbank Glaciers; also completion of Butson Ridge and Centre Island geology field work.- Unpubl. Rep. British Antarctic Survey, BAS. Reference No: G3/1970/E, Cambridge.

Smith, A.M., Vaughan, D.G., Doake, C.S.M. & Johnson, A.C. (1998): Surface lowering of the ice ramp at Rothera Point, Antarctic Peninsula, in response to regional climate change.- Ann. Glaciol. 27: 113-118.

Smith, R.C. & Stammerjohn, S.E. (1996): Surface air temperature variations in the western Antarctic Peninsula region.- In: R.M. ROSS, E.E. HOFMANN & L.B. QUENTIN (eds.), Foundations for ecological research west of the Antarctic Peninsula, AGU Ant. Res. Ser. 70: 105-121.

Steffen, K. (1995): Surface energy exchange at the equilibrium line on the Greenland ice sheet during onset of melt.- Ann. Glaciol. 21: 13-18.

Turner, J., Colwell, S.R. & Harangozo, S.A. (1997): Variability of precipitation over the western Antarctic peninsula from synoptic observations.- J. Geophys. Res. 102: 13999-14007.

Turner, J., Lachlan-Cope, T.A., Thomas, J.P. & Colwell, S.R. (1995): The synoptic origins of precipitation over the Antarctic Peninsula.- Ant. Sci. 7: 327-337.

Vaughan, D.G. & Doake, C.S.M. (1996): Recent atmospheric warming and retreat of ice shelves on the Antarctic Peninsula.- Nature 379: 328-330.

Warrick, R.A., Le Provost, C., Meier, M.F., Oerlemans, J. & Woodwort, P.L. (1996): Changes in sea level.-. In: J.T. HOUGHTON, L.G. MEIRA FILHO, B.A. CALLANDER, N. HARRIS, A. KATTENBERG & K. MASKELL (eds.), Climate Change 1995, The Science of Climate Change, IPCC Report, Cambridge University Press, Cambridge, 363-398.

Wunderle, S. (1996): Die Schneedeckendynamik der Antarktischen Halbinsel und ihre Erfassung mit aktiven und passiven Fernerkundungsverfahren.- Freiburger Geogr. Hefte, 48, Institut für Physische Geographie, Universität Freiburg, Germany, Freiburg.

Wunderle, S. & Schmidt, J. (1997). Glacier velocity determined by ERS-tandem data - A case study of the Antarctic Peninsula.- EARSeL Adv. Rem. Sens. 5: 64-70.